Knowledge-Based Systems 37 (2013) 415–426

Contents lists available at SciVerse ScienceDirect

Knowledge-Based Systems

journal homepage: www.elsevier.com/locate/knosys

A sub-block-based eigenphases algorithm with optimum sub-block size

Gibran Benitez-Garcia, Jesus Olivares-Mercado, Gabriel Sanchez-Perez, Mariko Nakano-Miyatake, Hector Perez-Meana *

Mechanical and Electrical Engineering School, National Polytechnic Institute of Mexico, Av. Santa Ana 1000, 04430 Mexico D.F., Mexico

ARTICLE INFO

Article history:
Received 2 February 2012
Received in revised form 4 May 2012
Accepted 31 August 2012
Available online 3 October 2012

Keywords:
Face recognition
Eigenphases
Sub-block processing
PCA
SVM
Partial occlusion

ABSTRACT

Several algorithms have been proposed for constrained face recognition applications. Among them the eigenphases algorithm and some variations of it using sub-block processing, appears to be desirable alternatives because they achieves high face recognition rate, under controlled conditions. However, their performance degrades when the face images under analysis present variations in the illumination conditions as well as partial occlusions. To overcome these problems, this paper derives the optimal sub-block size that allows improving the performance of previously proposed eigenphases algorithms. Theoretical and computer evaluation results show that, using the optimal block size, the identification performance of the eigenphases algorithm significantly improves, in comparison with the conventional one, when the face image presents different illumination conditions and partial occlusions respectively. The optimal sub-block size also allows achieving a very low false acceptance and false rejection rates, simultaneously, when performing identity verification tasks, which is not possible to obtain using the conventional approach; as well as to improve the performance of other sub-block-based eigenphases methods when rank tests are performed.

1. Introduction

Face recognition is one of the most widely used biometric recognition methods because it is the usual way used for most people to recognize another person. Additionally the data acquisition method for face recognition is non-intrusive because it consists only in taking a picture, which can be carried out with or without cooperation of the person to be recognized. These facts do the face recognition one of the biometric methods with higher acceptance among the users [1–3].

The face recognition as well as other biometric systems can be used for either, identity verification and person identification, depending on the data set used during the training stage. That is the reason why it is important to clarify the differences among these two tasks. In the first case, the system is asked to determine if the person is who he/she claims to be, while during the identification task, the system is asked to determine the person, among a set of persons whose face characteristics are stored in the database, that more closely resembles the image under analysis. Thus the recognition task encompasses both identification and verification [4,5].

Fig. 1 shows the block diagram of a general face recognition system, in which during the training stage, firstly the face image is obtained. Subsequently in the feature extraction stage a set of relevant and near invariant features of the face image are extracted to generate a template of the person under analysis. During the recognition operation, depending on the required task, slightly different processes are performed. Thus if the system is required to perform a verification task, besides the face image of the person under analysis, the identity of the user must be provided, in order to compare the estimated template of the person under analysis with the template of the person who he/she claims to be in order to take a decision; while if the system is required to perform an identification task, it is necessary to provide the face image of the person to be identified in order to estimate the template (live-template) of the person under analysis and compare it with all stored templates in the database, in order to determine the user identity.

In any face recognition system, the feature extraction stage plays a fundamental role because it is responsible for estimating a set of reduced and almost invariant parameters that allows eliminating the influence of variations related to hair style, illumination changes and partial occlusion; while maximizing the difference between faces of different people [6–10]. Thus the effectiveness of a face recognition system strongly depends on the performance of the algorithm used in the feature extraction stage. Because of that during the last two decades, several feature extraction algorithms have been proposed that intend to meet the requirements of providing a smaller intra-person variability and larger inter-person variability. Because the effect of an efficient feature extraction

* Corresponding author. Fax: +52 55 5656 2058.
E-mail addresses: mnakano@ipn.mx (M. Nakano-Miyatake), hmpm@prodigy.net.mx, hmperezm@ipn.mx (H. Perez-Meana).

0950-7051/$ - see front matter © 2012 Elsevier B.V. All rights reserved.
http://dx.doi.org/10.1016/j.knosys.2012.08.023

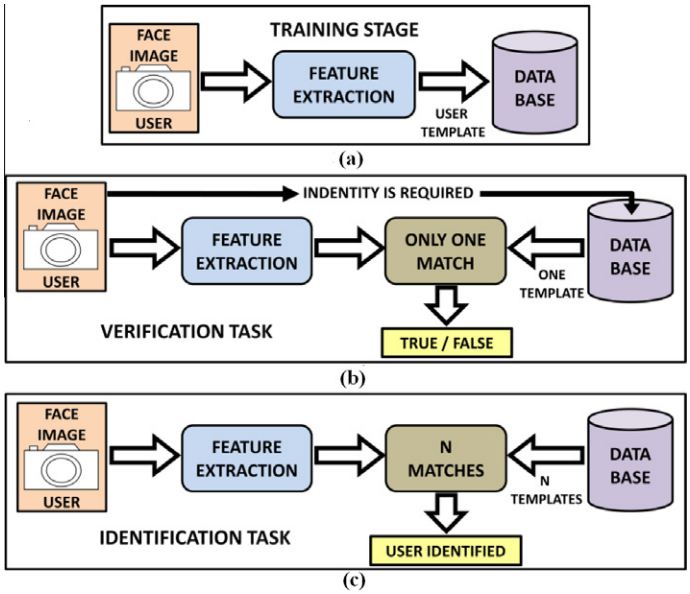

Fig. 1. General block diagram of face recognition system. (a) Training stage obtains the templates and stores them in the database. (b) Verification task, which determines if the person is who he/she claims to be. (c) Identification task that determines the identity of the person under analysis among a set of known people.

scheme in the overall performance of any face recognition system, several schemes have been proposed in the literature. Thus the use of frequency transformations such as Discrete Cosine Transform [11–13], Discrete Gabor Transform [14–17], Discrete Wavelet Transform [18–20] and Haar Transform [21] have been proposed which provide recognition rates higher than 90%. In addition the use of Fisherfaces [22,23], eigenfaces which uses the Principal Component Analysis (PCA) [24,25], and the Eigenphases [26] which uses the phase component of Fourier spectrum and the PCA have been also proposed in the literature. All of them, providing reasonably high recognition rates under several practical conditions. Among them the Eigenphases algorithm appears to be an attractive alternative because it provides better results than other algorithms [27,28] with a reasonable computational complexity. The Eigenphases algorithm works in the frequency domain using the phase spectrum, according to the Oppenheim experiment, together with the PCA for feature extraction and dimensionality reduction [26].

The Eigenphases algorithm performs fairly well, although its performance degrades when the face images used during training and recognition tasks were captured under quite different lighting conditions, they have very low contrast or even the face images present some partial occlusions. To solve the problems due to variation on the illumination conditions, the use of several preprocessing stages, that are able to improve the face image quality, have been proposed to improve the eigenphases algorithm such as: the normalization of the pixels value [29,30], the histogram equalization (HE) [31] and the Contrast Limited Adaptive Histogram Equalization (CLAHE) [32]. In all cases some improvement has been achieved compared with the original eigenphases method. In these works it is also shown that if the face image is split into several sub-blocks, before applying the preprocessing and feature extraction algorithm, some additional improvement is achieved; although they do not provide a theoretical explanation about it or a theoretical criterion about the optimal sub-block size selection.

This paper presents a complete analysis of the effect of using sub-block processing in the eigenphases algorithm providing a criterion about the optimal sub-block size selection. The analysis provided shows that it is important to divide the face image in sub-blocks and estimate the phase spectrum of each sub-block, independently, before applying the PCA; because, doing it, the performance of the sub-block-based eigenphases algorithm becomes almost independent of the illumination condition. The sub-block-based eigenphases algorithm and conventional one are evaluated in a controlled environment with a uniform background, using the AR Face Database. It is important to emphasize that, although recently the interest in developing unconstrained face recognition algorithms has been growing, the face recognition systems operating in controlled environments have still a large number of applications such as access control and development of ID cards etc. Theoretical and computer evaluation results show that using the sub-block-based eigenphases algorithm with the optimal block size, 2×2 pixels, the identification is improved about 3%, in comparison with the conventional one, when the face image presents different illumination conditions and facial expression, and about 12% when it presents partial occlusions; while when the sub-block-based eigenphases algorithm with optimal sub-block is required to perform identity verification tasks, it is able to provide, simultaneously, false acceptance and false rejection rates lower than 0.5%, which is not possible to obtain using the conventional approach.

The rest of the paper is organized as follows: Section 2 provides a description of the sub-block-based eigenphases algorithm. Section 3 provides a theoretical analysis of the sub-block processing effect in the performance of eigenphases algorithm and shows that the optimum sub-block size is 2×2 pixels. Section 4 provides detailed evaluation results. Finally Section 5 provides the conclusions of this work.

2. Sub-block-based eigenphases algorithm

The block diagram of the sub-block-based eigenphases algorithm, shown in Fig. 2, includes the option of using a preprocessing stage, which may be used to reduce the variation of the pixels value due to change on the illumination conditions, before the phase spectrum and PCA estimation. The same face recognition system, changing only the classifier stage, can perform both, the identification and verification tasks. This is because, firstly, during the training the classifier stage generates the templates for each user saving

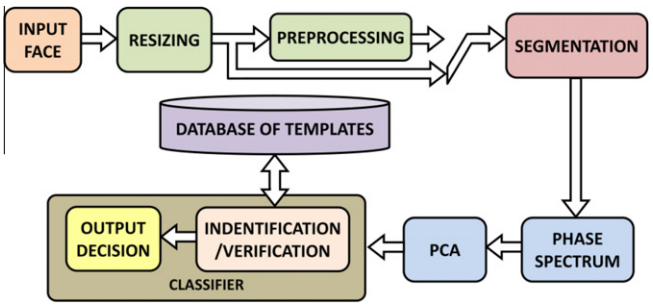

Fig. 2. Block diagram of proposed face recognition algorithm.

them in a database. Next when the system is required to perform a face identification task the classifier compares the template of the person under analysis with all templates in the database to determine the identity of the person under analysis, while to perform an identity verification task the template of the person under analysis is compared with the template of the person who he/she claims to be.

The sub-block-based eigenphases algorithm, firstly, captures the face image of the person under analysis and downsamples it in order to reduce the number of operations required to calculate the PCA. The downsampled image is given by

$$I(n,m) = I_{input}(nT_s, mT_s) \tag{1}$$

where I_{input} is the face image under analysis, T_s is the downsampling factor and I is the downsampled image. Next, the downsampled image may be fed into a preprocessing stage to improve the image feature estimation using pixel normalization, histogram equalization or CLAHE, etc. Subsequently the face image is divided in $L \times M$ sub-blocks of size $N \times N$ whose phase spectrum is independently estimated. After the estimation of phase spectrum of each sub-block, the resulting matrices are concatenated before applying the PCA, which is used for dimensionality reduction and extraction of the relevant information of the face image under analysis to form the estimated template. Finally using the estimated template a classifier, such as the Support Vector Machine (SVM), is trained to perform either the identification or verification task. During face recognition operation, the classifier determines the more possible identity of the person under analysis or if the person under analysis is who he/she claims to be, depending on whether the system is performing identification or verification tasks. Fig. 3 shows the output of each one of the first five stages of the sub-block-based eigenphases algorithm. The input face image is shown in Fig. 3a and b is the image after the downsampling process, Fig. 3c is the result obtained when the CLAHE algorithm is applied to the input image Fig. 3b, which may be omitted. The image Fig. 3d is the result of the image segmentation in $L \times M$ sub-blocks, and Fig. 3e is the matrix obtained by concatenating the phase spectrum of each sub-block of Fig. 3d.

2.1. Preprocessing stage

In previous works, it has been proposed to use several preprocessing stage to improve the performance of face recognition when the face images are obtained under different illumination and background conditions [29–32]. The purpose of the preprocessing stage is to modify the face image such that the variations of the image characteristics, due to the illumination condition, are kept as smaller as possible, to increase the accuracy of the feature extraction in the next stages. Several methods to achieve this goal have been proposed such as the histogram equalization, the CLAHE as well as the normalization of the image pixels value. The pixels value normalization is used as preprocessing stage in the algorithm proposed in [29,30], this method generates a certain independence of image properties which are the brightness, contrast and background. The pixel normalization used in [29,30], consists on dividing each pixel by the mean square value of the given sub-block.

The histogram equalization [33] is an image enhancement processing for increasing the contrast, transforming the original image histogram into an approximately uniform one. That is, making the distribution intensity of the image pixels approximately uniform. The use of histogram equalization process in the preprocessing stage was proposed in [31]. In general this method performs well, however it presents some problems when the face images have some regions with good contrast and other regions with very low-contrast. This problem can be solved by using the Contrast Limited Adaptive Histogram Equalization (CLAHE) [34–37] which was used as preprocessing stage in [32]. Fig. 4 shows the result of applying the preprocessing algorithms mentioned above, where (a) is the input face image, (b) shows the result to apply CLAHE, (c) shows the result to apply the histogram equalization and (d) is the result to apply pixel value normalization.

2.2. Segmentation

To improve performance of eigenphases algorithm, the face image under analysis is split into several sub-blocks. These sub-blocks are firstly processed, as mentioned above, before estimating the phase spectrum of each sub-block, independently [29–32]. Next the phase spectrums of all blocks are concatenated, as shown in Fig. 3, before PCA estimation. This approach has been successfully used with sub-blocks of size 12×12, 6×6, 3×3 pixels. However, despite the sub-block processing improves the performance of eigenphases algorithm, any of these references provide a criterion to select the optimal sub-block size.

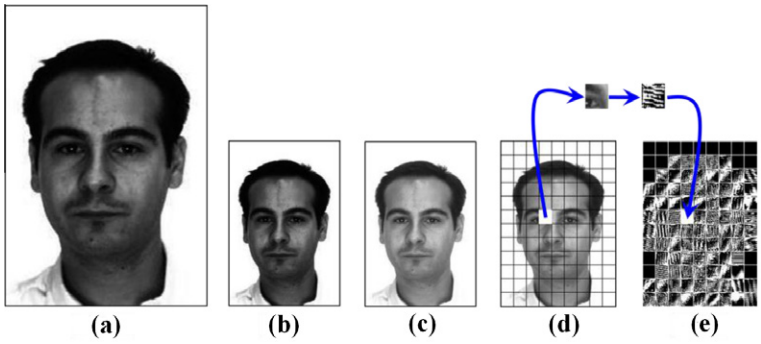

Fig. 3. Example of the application of first five stages of the proposed algorithm. (a) Original face image. (b) Downsampled image. (c) Face image after use CLAHE method in (b). (d) Face image divided in sub-blocks. (e) Concatenation of the phase spectrum of each sub-block of (d).

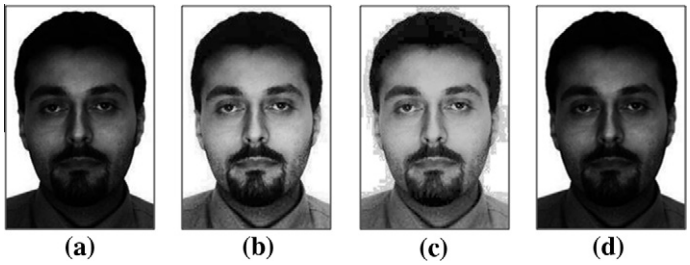

Fig. 4. Example results of the three algorithms used in the preprocessing stage. (a) Input face image. (b) Result to apply CLAHE. (c) Result to apply histogram equalization. (d) Result to apply pixel normalization value.

2.3. Phase spectrum

The sub-block-based eigenphases algorithm is based on the Oppenheim experiment [38], which shows that the phase spectrum of a face image contains more relevant information than its magnitude [39]. This is illustrated in the experiment shown in Fig. 5, in which firstly the Fourier transform of two different images is calculated. Then, the face 1 (a) is reconstructed using the phase spectrum of face 1 (c) and the magnitude spectrum of face 2 (f); and the face 2 (e) is reconstructed using the phase spectrum of face 2 (g) and the magnitude spectrum of face 1 (b). The reconstructed images, (d) and (h), show that the synthesized face images clearly resemble face 1 (a) and face 2 (e), respectively.

As mentioned in Section 2.2, the face image is segmented in $L \times M$ blocks of $N \times N$ pixels, where $NL \times NM$ is the image size. This process is applied to the downsampled image with or without preprocessing. The phase spectrum of each sub-block is estimated as follows:

$$\varphi_{j,k} = \tan^{-1}\left(\frac{Im(FFT(I_{j,k}(m,n)))}{Re(FFT(I_{j,k}(m,n)))}\right), \quad m,n = 1,2,\ldots N \tag{2}$$

where $I_{j,k}(m,n)$ is the (j,k)th sub-block of face image obtained in the segmentation stage. Next the phase spectrums of all sub-blocks are concatenated, that is:

$$\varphi = \begin{bmatrix} \varphi_{1,1} & \varphi_{1,2} & \cdots & \varphi_{1,M} \\ \varphi_{2,1} & \varphi_{2,2} & \cdots & \varphi_{2,M} \\ \cdots & \cdots & \cdots & \cdots \\ \varphi_{N,1} & \varphi_{N,2} & \cdots & \varphi_{N,M} \end{bmatrix} \tag{3}$$

where φ is the phase spectrum matrix used by the PCA stage for feature vector estimation. Fig. 6 shows the process of extracting the phase spectrum by sub-block segmentation, where (a) and (b) show the phase spectrum matrix φ estimated using sub-blocks of size 12×12 and 6×6 pixels, respectively.

2.4. Principal Components Analysis (PCA)

The PCA is a standard tool in modern data analysis widely used in diverse fields from neuroscience to computer graphics, because it is an efficient, non-parametric method for extracting relevant information from confusing datasets [40–43]. The other main advantage of PCA is reduction of dimensionality of extracted data without much loss of information. This technique is used to extract the most relevant features of the face image [44].

The procedure to develop the PCA analysis of input images is, firstly consider ϕ, whose ith row corresponds to the feature vector of the ith training image, φ_i given by Eq. (3) is stored in a vector of size $M_r = L \times M \times N^2$ given by:

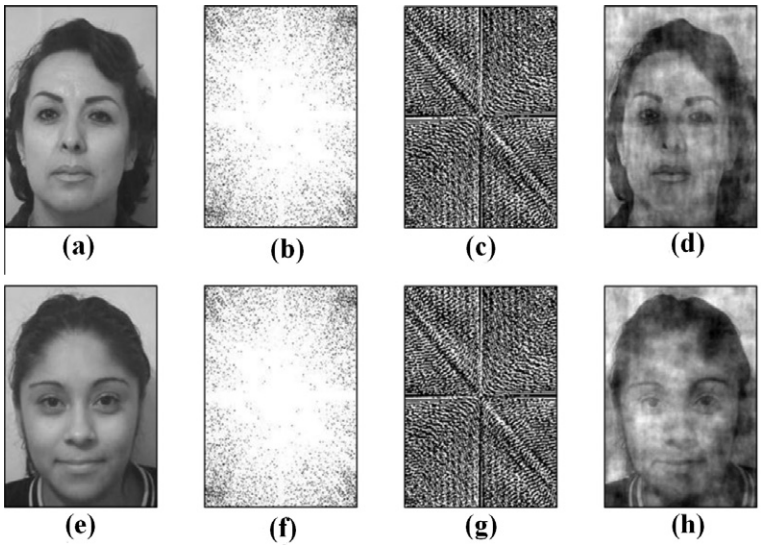

Fig. 5. Oppenheim's experiment. (a) Image of face 1. (b) Magnitude spectrum of face 1. (c) Phase spectrum of face 1. (d) Reconstructed image using (c) and (f). (e) Image of face 2. (f) Magnitude spectrum of face 2. (g) Phase spectrum of face 2. (h) Reconstructed image using (b) and (g).

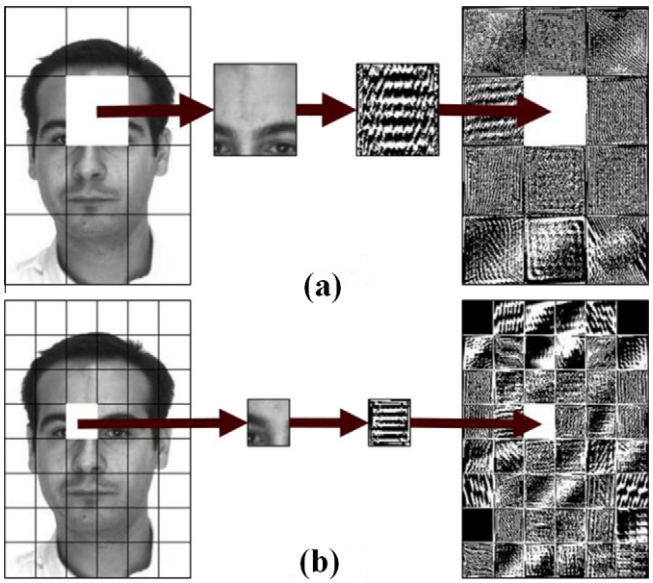

Fig. 6. Example of the phase spectrum extraction of same face input image using different sub-block size. (a) Phase spectrum estimation using sub-blocks of 12×12 pixels. (b) Phase spectrum estimation using sub-blocks of 6×6 pixels.

$$\phi^i = \begin{bmatrix} \phi_0^i & \phi_1^i & \dots & \phi_{M_r-1}^i \end{bmatrix} \tag{4}$$

where
$\phi_r^i = \varphi_{p,q}^i,\ r = pq,\ p = jN + m_1,\ q = kN + m_2,\ 0 \leqslant m_1, m_2 \leqslant N-1$
and $L \times M$ is the number of blocks and N^2 is the number of pixels in each block. Thus ϕ is given by:

$$\phi = \begin{bmatrix} \phi_0^0 & \phi_0^1 & \dots & \phi_0^{P-1} \\ \phi_1^0 & \phi_1^1 & \dots & \phi_1^{P-1} \\ \vdots & \vdots & \vdots & \vdots \\ \phi_{M_r-1}^0 & \phi_{M_r-1}^1 & \dots & \phi_{M_r-1}^{P-1} \end{bmatrix} \tag{5}$$

where P is the total number of images used for training. Next, subtracting the average image from each training image it follows that

$$\hat{\phi} = \begin{bmatrix} \phi_0^0 - \bar{\phi}_0 & \phi_0^1 - \bar{\phi}_0 & \dots & \phi_0^{P-1} - \bar{\phi}_0 \\ \phi_1^0 - \bar{\phi}_1 & \phi_1^1 - \bar{\phi}_1 & \dots & \phi_1^{P-1} - \bar{\phi}_1 \\ \vdots & \vdots & \vdots & \vdots \\ \phi_{M_r-1}^0 - \bar{\phi}_{M_r-1} & \phi_{M_r-1}^1 - \bar{\phi}_{M_r-1} & \dots & \phi_{M_r-1}^{P-1} - \bar{\phi}_{M_r-1} \end{bmatrix} \tag{6}$$

where

$$\bar{\phi}_n = \frac{1}{P}\sum_{n=0}^{P-1} \phi_n^i \tag{7}$$

Next, the eigenvalues of the covariance matrix:

$$\Omega = \hat{\phi}^T \hat{\phi} \tag{8}$$

are estimated which has up to P eigenvectors associated with non-zero eigenvalues, where $P < M_r$, that are then stored in a descendent order according to the corresponding eigenvalues. The stored eigenvectors of the covariance matrix Ω are:

$$\mathbf{V} = \left[\mathbf{V}_0^T, \mathbf{V}_1^T, \dots, \mathbf{V}_{P-1}^T\right]^T \tag{9}$$

where $\mathbf{V}_0$ is the eigenvector associated with the largest eigenvalue λ_0, $\mathbf{V}_1$ is the eigenvector associated with the second largest eigenvalue λ_1 and so on. Next, consider that the eigenvectors of matrix $\hat{\phi}\hat{\phi}^T$ stored in a descendent order according to corresponding eigenvalues,

$$\boldsymbol{\psi} = [\boldsymbol{\psi}_0, \boldsymbol{\psi}_1, \dots.., \boldsymbol{\psi}_{P-1}] \tag{10}$$

which can be estimated using the eigenvectors $\mathbf{V}_k$, as follows

$$\boldsymbol{\psi}_k^T = \frac{\hat{\phi}\mathbf{V}_k}{\sqrt{\lambda_k}} \tag{11}$$

where $\hat{\phi}$ is a matrix of size $M_r \times P$ given by Eq. (6), $\mathbf{V}_k$ is the kth eigenvector of $\boldsymbol{\Omega}$ of size P, and P is the number of images used for training. Thus the reduced space feature vector $\boldsymbol{Y}$ is given by

$$\mathbf{Y} = \boldsymbol{\psi}\phi^T \tag{12}$$

where $\boldsymbol{\psi}$ is a $M_r \times P$ matrix whose kth row, given by Eq. (10), is the kth eigenvector of matrix $\hat{\phi}\hat{\phi}^T$. Fig. 7 shows the process to generate the feature vectors. Firstly the phase spectrums of training images are converted into column vectors and then these vectors form a matrix ϕ. Next the principal components were extracted from ϕ to generate a matrix of dominant features $\boldsymbol{\psi}$. Finally the column vector of each training image is multiplied by $\boldsymbol{\psi}^T$ to generate a feature vector $\boldsymbol{Y}$, subsequently these vectors are used to characterize the image under analysis.

2.5. Classifier

After the feature vector is estimated, to perform the identification or verification task, a Support Vector Machine (SVM) [45,46] is used. During training, the SVM is responsible for generating the templates for each person. When the SVM is required to perform a verification task, the SVM is trained such that its output becomes closer to one when the person is who he/she claims to be and close to zero in other case. This task is carried out using only one template of the database and a given threshold. On the other hand, when the SVM is used to perform an identification task, it is trained such that its larger output corresponds to the most likely person, using all templates of database. In this paper the LIBSVM library [47] is used, where the characteristics used for training and recognition tasks are: Kernel type: polynomial: (gamma*u'*v + coef0)^degree, where coef0 = 1, gamma = 1, cost = 100, and all others parameters are used with their default values given by the LIBSVM [47].

The objective of the SVM, which is a universal constructive learning procedure for pattern recognition based on the statistical learning theory, is assigned to each pattern a class [48–50] as described as follows: assume there is a set of points belonging to two different classes. Intuitively, a SVM finds the hyper-plane that separates the largest possible fraction of points of the same class such that they are in the same side of the hyper-plane, while

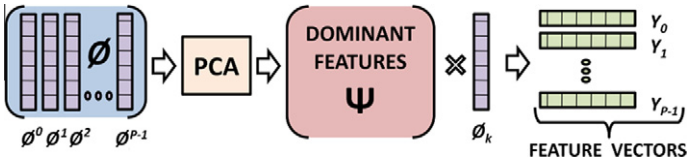

Fig. 7. Process to generate the feature vector using PCA.

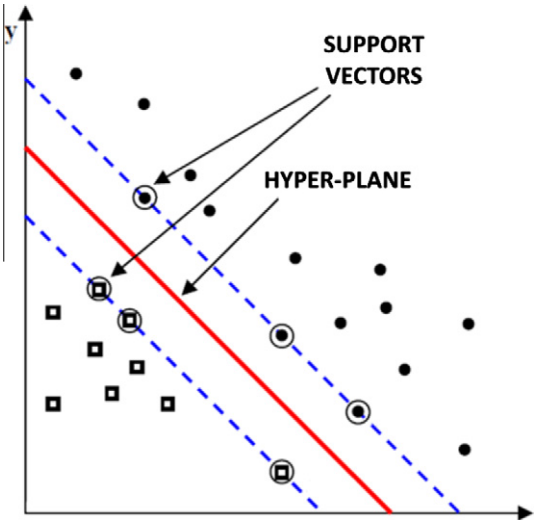

Fig. 8. Classification between two classes using SVM.

minimizing the distance between both classes and the hyper-plane. For a two-class classification problem, shown in Fig. 8, the goal is to separate the two classes by a hyper-plane estimated from the available samples. This figure shows the result of the separation of two classes using the SVM, where the distance between the hyper-plane and the nearest data point of each class is kept to a minimum.

3. Optimum sub-block size

Several modifications of the eigenphases algorithm have been proposed which segment the face image under analysis into several sub-blocks of size $N \times N$, before the phase spectrum estimation [29–32]. However, they do not report how to obtain the optimal block size. To obtain the optimal block size, consider a given sub-block, $f(t_1, t_2)$, $0 \leqslant t_1 \leqslant NT$, $0 \leqslant t_2 \leqslant MT$ and assume that is a separable function, i.e. $f(t_1,t_2) = f_1(t_1)f_2(t_2)$, where $f_1(t_1)$ and $f_2(t_2)$ can be approximated using a piecewise approach as shown in Fig. 9. Then, the Fourier transform of sub-block $f(t_1, t_2)$ is given by

$$\begin{aligned} F(\omega_1,\omega_2) &= \int_0^{NT}\int_0^{MT} f_1(t_1,t_2)e^{-j\omega_1 t_1}e^{-j\omega_2 t_2}dt_1dt_2 \\ &= \int_0^{NT} f_1(t_1)e^{-j\omega_1 t_1}dt_1 \int_0^{MT} f_2(t_2)e^{-j\omega_2 t_2}dt_2 \end{aligned} \tag{13}$$

where N and M are the number of pixels in each row and column, respectively, and T is the separation between two consecutive pixels in any given sub-block. Assuming that T is small enough, Eq. (13) can be approximated as

$$\begin{aligned} F(\omega_1,\omega_2) &= F_1(\omega_1)F_2(\omega_2) \\ &= \sum_{n=0}^{N-1}\int_{nT}^{(n+1)T}\left(\frac{k_nA_n}{T}t_1 + A_n(1-nk_n)\right)e^{-j\omega_1 t_1}dt_1 \\ &\quad\times\sum_{m=0}^{M-1}\int_{mT}^{(m+1)T}\left(\frac{k_mA_m}{T}t_2 + A_m(1-mk_m)\right)e^{-j\omega_2 t_2}dt_2 \end{aligned} \tag{14}$$

Next, defining

$$\begin{aligned} G_n(\omega_1) &= \int_{nT}^{(n+1)T}\left(\frac{k_nA_n}{T}t_1 + A_n(1-nk_n)\right)e^{-j\omega_1 t_1}dt_1 \\ &= \int_{nT}^{(n+1)T}\frac{k_nA_n}{T}t_1e^{-j\omega_1 t_1}dt_1 + \int_{nT}^{(n+1)T}A_n(1 \\ &\quad - nk_n)e^{-j\omega_1 t_1}dt_1 \end{aligned} \tag{15}$$

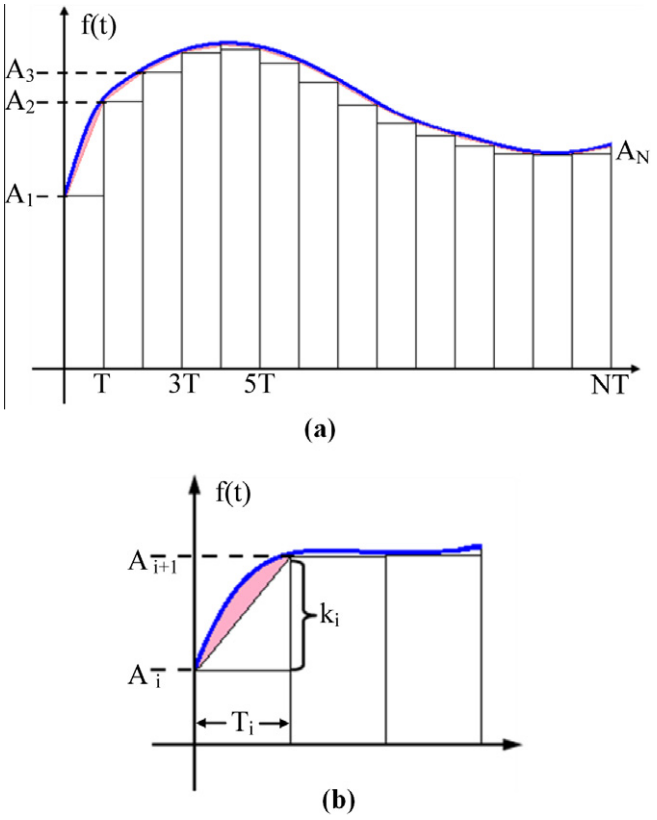

Fig. 9. (a) Piecewise approach of a column or row of a given sub-block $f(t_1,t_2)$ of input image. (b) Detailed representation of ith section.

After some manipulations, assuming without loss of generality that $T = 1$, Eq. (15) becomes

$$\begin{aligned} G_n(\omega_1) &= k_nA_n\left(\frac{(n+1)}{\omega_1}\sin((n+1)\omega_1) - \frac{n}{\omega_1}\sin(n\omega_1)\right. \\ &\quad\left. + \frac{1}{\omega_1^2}\cos((n+1)\omega_1) - \frac{1}{\omega_1^2}\cos(n\omega_1)\right) \\ &\quad + 2A_n(1-nk_n)\sin\left(\frac{\omega_1}{2}\right)\cos\left(\left(n+\frac{1}{2}\right)\omega_1\right) \\ &\quad + jk_nA_n\left(\frac{(n+1)}{\omega_1}\cos((n+1)\omega_1) - \frac{n}{\omega_1}\cos(n\omega_1)\right. \\ &\quad\left. - \frac{1}{\omega_1^2}\sin((n+1)\omega_1) + \frac{1}{\omega_1^2}\sin(n\omega_1)\right) \\ &\quad - j2A_n(1-nk_n)\sin\left(\frac{\omega_1}{2}\right)\sin\left(\left(n+\frac{1}{2}\right)\omega_1\right) \end{aligned} \tag{16}$$

Finally from Eq. (14) it follows that $F_1(\omega_1)$ is given by

$$F_1(\omega_1) = \sum_{n=0}^{N-1}\left(G_n^R(\omega_1) + jG_n^I(\omega_1)\right) \tag{17}$$

where

$$\begin{aligned} G_n^R(\omega_1) &= Re\{G_n(\omega_1)\} \\ &= k_nA_n\left(\frac{(n+1)}{\omega_1}\sin((n+1)\omega_1) - \frac{n}{\omega_1}\sin(n\omega_1)\right. \\ &\quad\left. + \frac{1}{\omega_1^2}\cos((n+1)\omega_1) - \frac{1}{\omega_1^2}\cos(n\omega_1)\right) \\ &\quad + 2A_n(1-nk_n)\sin\left(\frac{\omega_1}{2}\right)\cos\left(\left(n+\frac{1}{2}\right)\omega_1\right) \end{aligned} \tag{18}$$

$$G_n^I(\omega_1) = Im\{G_n(\omega_1)\} = k_n A_n \left(\frac{(n+1)}{\omega_1} \cos((n+1)\omega_1) - \frac{n}{\omega_1} \cos(n\omega_1) - \frac{1}{\omega_1^2} \sin((n+1)\omega_1) + \frac{1}{\omega_1^2} \sin(n\omega_1) \right) - 2A_n(1 - nk_n) \sin\left(\frac{\omega_1}{2}\right) \sin\left(\left(n+\frac{1}{2}\right)\omega_1\right) \quad (19)$$

In a similar form, it follows that the Fourier transform of column of the image, $F_2(\omega_2)$ is given by

$$F_2(\omega_2) = \sum_{m=0}^{N-1} \left(G_m^R(\omega_2) + jG_m^I(\omega_2) \right) \quad (20)$$

where

$$G_m^R(\omega_2) = Re\{G_m(\omega_2)\} = k_m A_m \left(\frac{(m+1)}{\omega_2} \sin((m+1)\omega_2) - \frac{m}{\omega_2} \sin(m\omega_2) + \frac{1}{\omega_2^2} \cos((m+1)\omega_2) - \frac{1}{\omega_2^2} \cos(m\omega_2) \right) + 2A_m(1 - mk_m) \sin\left(\frac{\omega_2}{2}\right) \cos\left(\left(m+\frac{1}{2}\right)\omega_2\right) \quad (21)$$

$$G_m^I(\omega_2) = Im\{G_m(\omega_2)\} = k_m A_m \left(\frac{(m+1)}{\omega_2} \cos((m+1)\omega_2) - \frac{m}{\omega_2} \cos(m\omega_2) - \frac{1}{\omega_2^2} \sin((m+1)\omega_2) + \frac{1}{\omega_2^2} \sin(m\omega_2) \right) - 2A_m(1 - mk_m) \sin\left(\frac{\omega_2}{2}\right) \sin\left(\left(m+\frac{1}{2}\right)\omega_2\right) \quad (22)$$

Then, from Eqs. (14), (17) and (20) it follows that

$$F_1(\omega_1, \omega_2) = F_1(\omega_1) F_2(\omega_2) = \sum_{n=0}^{N-1} \left(G_n^R(\omega_1) + jG_n^I(\omega_1) \right) \sum_{m=0}^{N-1} \left(G_m^R(\omega_2) + jG_m^I(\omega_2) \right) \quad (23)$$

Finally, from Eq. (23) the phase of $F(\omega_1,\omega_2)$ is given by

$$\theta(\omega_1, \omega_2) = \tan^{-1} \frac{\sum_{n=0}^{N-1} G_n^I(\omega_1)}{\sum_{n=0}^{N-1} G_n^R(\omega_1)} + \tan^{-1} \frac{\sum_{m=0}^{N-1} G_m^I(\omega_2)}{\sum_{m=0}^{N-1} G_m^R(\omega_2)} \quad (24)$$

Thus, from Eq. (24) it follows that, if the block size used for feature extraction contains only two samples, that is if $N = 1$, the effect of the magnitude of pixels, A_n and A_m in Eqs. (18)–(24), disappears depending only in the value of k_n and k_m, such that the phase of Fourier spectrum of the sub-block under analysis becomes

$$\theta(\omega_1, \omega_2) = \tan^{-1} \left[\frac{\left(\omega_1 k_n \cos(\omega_1) - k_n \sin(\omega_1) - 2\omega_1^2 \sin^2(\omega_1/2) \right)}{(\omega_1 k_n \sin(\omega_1) + k_n \cos(\omega_1) - \omega_1^2 \sin(\omega_1) - k_n)} \right] + \tan^{-1} \left[\frac{\left(\omega_2 k_m \cos(\omega_2) - k_m \sin(\omega_2) - 2\omega_2^2 \sin^2(\omega_2/2) \right)}{(\omega_2 k_m \sin(\omega_2) + k_m \cos(\omega_2) - \omega_2^2 \sin(\omega_2) - k_m)} \right] \quad (25)$$

Then from Eq. (25) it follows that we can conclude that the optimum block size that provides the highest robustness of the sub-block-based eigenphases algorithm to illumination changes is equal to 2×2, as shown in Fig. 10.

Fig. 10 shows an experiment where the phase spectrum of two images with different illumination conditions are calculated, using several sub-block sizes; together with the difference between phase spectrums of these two images. From this figures it follows that the difference between both phase spectrums is very small and then the illumination effect becomes almost negligible when sub-block size becomes smaller. Fig. 1: (a) is a face image with normal illumination; (b) is a face image with low illumination; (c–e) show the result obtained using sub-blocks of 12×12, 4×4 and the optimum one, i.e. 2×2 pixels, respectively, together with the difference between the phase spectrums of (a) and (b) when both of them are segmented using the same sub-block size.

4. Evaluation results

In order to evaluate the performance of the sub-block-based eigenphases algorithm with optimum block size and compare it with the conventional methods, several computer evaluations have been realized under the same conditions in a controlled environment using "The AR Face Database" [51], which has been expanded to obtain a larger amount of illumination variations in the face pictures. This version of data base includes 12,000 face images of 120 persons (65 males and 55 females), which includes 100 samples of each person with several illumination variations; facial expressions and partial occlusion, consisting of face images of persons with sunglasses.

The face images included in the database have been divided into two different sets: the set A consisting of 70 images per person including images with illumination changes and different facial expressions and set the B which consists of 30 images per person that includes images with partial occlusion due to sunglasses and illumination changes. Some samples of the face images included in the sets A and B are shown in Fig. 11a and b, respectively. In all cases after the down sampling the image size becomes 48×36 pixels.

One important issue is the number of face images required for properly training of the recognition system. Thus, in order to determine the appropriate number of training images, the conventional and sub-block-based eigenphases methods, with optimum sub-block size, were evaluated using 1 to 14 training images. Based on the evaluation results, shown in Fig. 12, it follows that using the sub-block-based eigenphases methods, with optimum sub-block size, requires about 5 or 6 training images to achieve a good recognition performance, while the conventional method requires about 12 to achieve similar recognition rate. To find the identification rate, this test was performed using the set A. Seven of the 14 training images of one of the 120 different persons selected for this test are shown in Fig. 13.

4.1. Identification performance

The identification performances were evaluated, without preprocessing stage, using five different block sizes: complete image, where the phase spectrum is obtained from the whole image, as proposed in the conventional eigenphases algorithm [26]; and the sub-block-based method with sub-blocks of size 12×12, 6×6, 4×4 and 2×2 pixels, in which the phase spectrum is obtained independently for each sub-block. In addition three different preprocessing stages were used: pixel value normalization, histogram equalization and CLAHE. Table 1 shows the identification results using images of set A together with its standard deviation.

The evaluation results presented in Table 1 show that the highest identification rate and lowest standard deviation is obtained when a sub-block size of 2×2 pixels is used. These results show that the use of sub-blocks improves the performance of conventional eigenphases method. In particular the sub-block-based

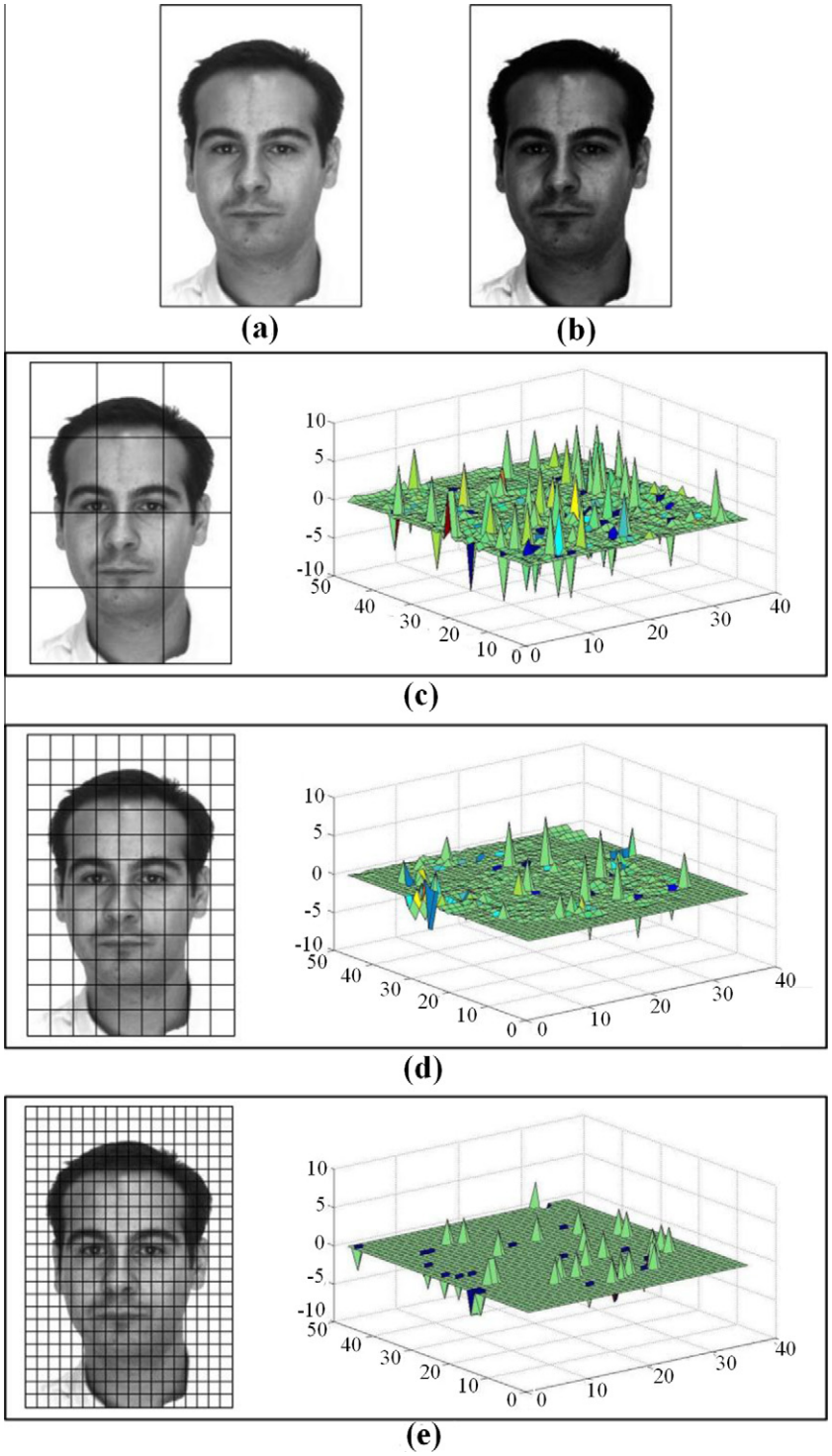

Fig. 10. Example of the differences between the phase spectrums of two images with different illumination conditions using sub-block segmentation. (a) Face image with normal illumination. (b) Face image with low illumination. (c) Difference of the phase spectrum obtained using sub-blocks of 12×12 pixels. (d) Difference of the phase spectrum obtained using sub-blocks of 4×4 pixels. (e) Difference of the phase spectrum obtained using sub-blocks of 2×2 pixels.

method that uses the optimum block size provides an improvement of approximately 3%.

Fig. 14 shows the rank evaluation of sub-block-based system using sub-block size of 2×2, 6×6 pixels together with the conventional eigenphases algorithm that uses the complete image. The evaluation results show that the sub-block-based method, with optimum sub-block sizes, i.e. 2×2 pixels, reach 100% of the identification rate in a lower number of ranks compared with the previously proposed ones.

Any face recognition system often finds the problem of identify images with partial occlusion. Therefore the performance of sub-block-based system, with block size of 2×2, was also evaluated using face image with partial occlusion. Table 2 shows the results, under the same conditions as Table 1, obtained when the proposed

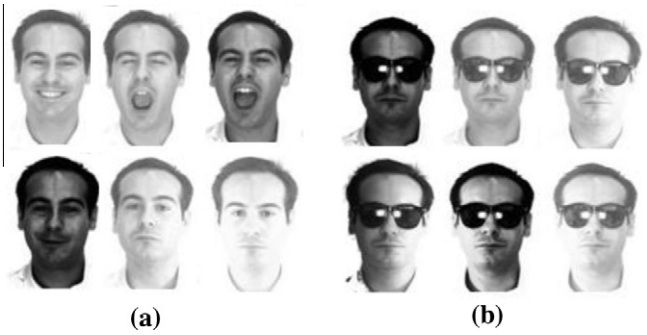

Fig. 11. Example of face images with illumination changes, facial expressions and partial occlusion included in (a) Set A, (b) Set B.

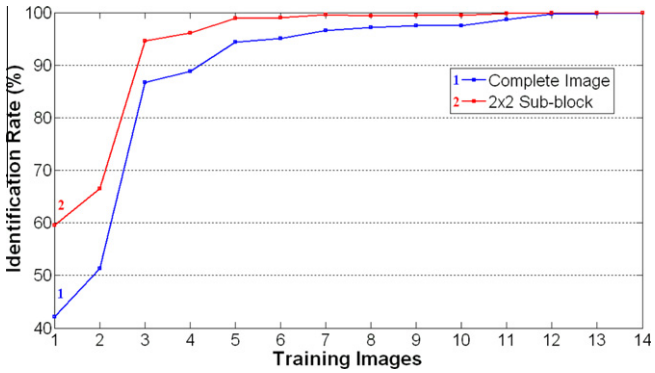

Fig. 12. Evaluation results using different number of training images. Using conventional eigenphases method and proposed algorithm with sub-blocks of 2×2 pixels, applied to images of set A.

system is evaluated applying the set B, while the SVM was trained using images without occlusion as shown in Fig. 11a. This approach is more realistic in practical application because the training images used are without occlusion and all test images present partial occlusion as shown in Fig. 11b.

It is important to mention that, again, according to the results of Table 2 the sub-block-based system performs better than the conventional eigenphases method. In particular the sub-block-based method with the optimum sub-block size provides an

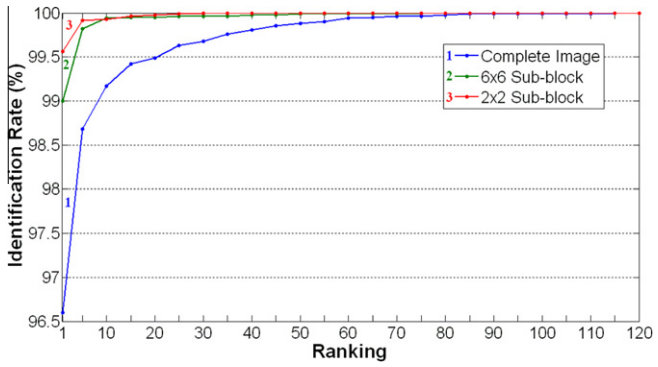

Fig. 14. Rank evaluation of proposed system using sub-block sizes of 6×6 and 2×2 pixels together with the conventional eigenphases method.

identification rate approximately 12% higher than the conventional eigenphases method, representing it a significant improvement. Also it is worth noting that even with significant partial occlusion in the testing images the performance of sub-block-based method with optimum block size, only degrades in approximately 2% compared with 11% of the conventional method. Fig. 15 shows the ranking evaluation of conventional eigenphases method and the sub-block-based one with sub-blocks of size 6×6 and 2×2 pixels using images of set B. Evaluation results clearly show that the sub-block-based algorithm with optimum block size, i.e. 2×2 pixels, provides better performance than the conventional one.

4.2. Identity verification performance

Any face verification system strongly depends on an appropriate selection of a threshold value to determine if the person under analysis is who she/he claims to be. To this end a detailed evaluation of the performance of sub-block-based systems was carried out to evaluate the false acceptance and false rejection rates as a function of the decision threshold. In all evaluations the preprocessing stage was omitted because, as shown in Section 3.1, its contribution is negligible when a sub-block processing is used.

Figs. 16–20 show the performance of the conventional eigenphases method, as well as the sub-block-based system when sub-block sizes of 12×12, 6×6, 4×4 and 2×2 pixels, is used in identity verification tasks with several different threshold values. These figures show that, as expected, the false acceptation

Fig. 13. Example of the training images used to evaluate the performance of proposed method.

Table 1
Identification rate and its standard deviation with different sub-block sizes and preprocessing using images of set A.

Block size	Without preprocessing		Histogram equalization		Normalization		CLAHE	
	Identification rate (%)	σ	Identification rate (%)	σ	Identification rate (%)	σ	Identification rate (%)	σ
Complete image	96.60	4.81	96.74	4.90	96.60	4.81	96.50	4.71
12×12	97.88	3.65	97.44	3.87	97.89	3.72	97.42	4.47
6×6	99.00	2.19	98.56	3.12	98.98	2.32	99.01	2.27
4×4	99.15	2.11	98.90	2.51	99.10	2.21	99.06	2.42
2×2 (optimum)	99.56	1.45	99.42	1.55	99.57	1.46	99.62	1.40

Table 2
Identification rate and its standard deviation with different sub-block sizes and preprocessing using images of set B.

Block size	Without preprocessing		Histogram equalization		Normalization		CLAHE	
	Identification rate (%)	σ	Identification rate (%)	σ	Identification rate (%)	σ	Identification rate (%)	σ
Complete image	85.44	19.49	83.17	19.43	85.44	19.44	84.81	19.87
12×12	87.83	17.22	83.31	18.56	88.00	17.12	86.58	16.52
6×6	93.08	15.22	90.89	15.37	93.03	15.19	92.50	14.59
4×4	95.00	12.05	94.00	11.71	94.92	11.93	95.17	11.80
2×2 (optimum)	97.19	9.56	96.56	10.70	97.33	9.21	97.03	9.84

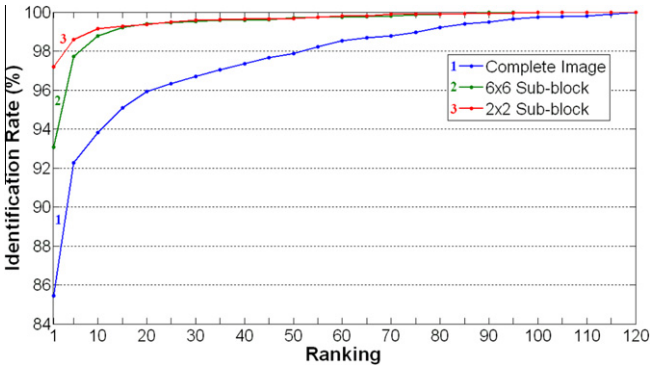

Fig. 15. Rank evaluation of proposed system using sub-block sizes of 6×6 and 2×2 pixels together with the conventional eigenphases method using set B.

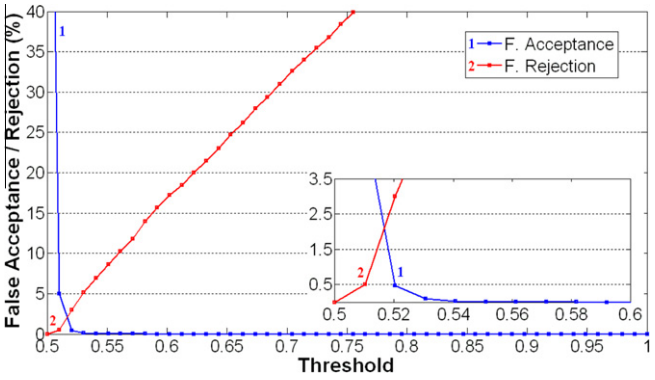

Fig. 16. False acceptance and false rejection rates provided by the conventional eigenphases method using images of set A.

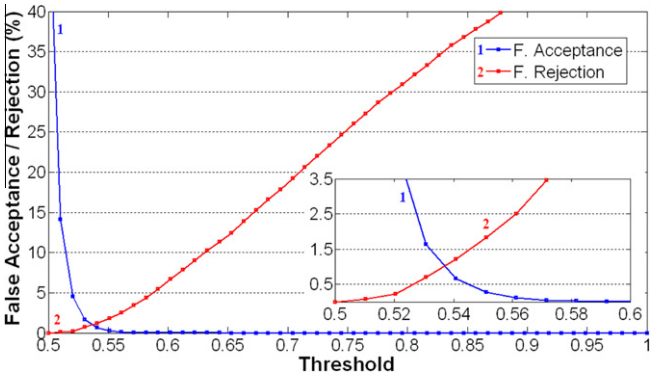

Fig. 17. False acceptance and false rejection rates provided by the proposed system using sub-block of 12×12 pixels applied to images of set A.

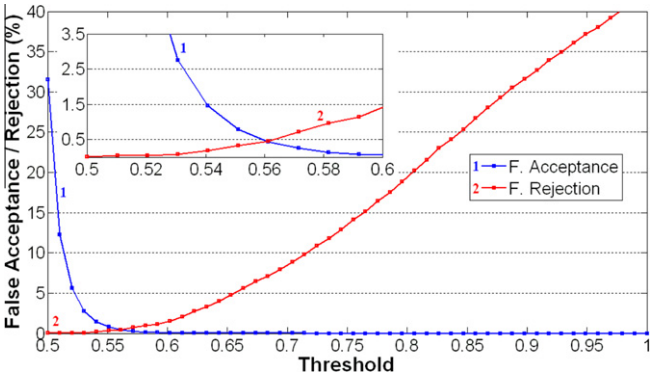

Fig. 18. False acceptance and false rejection rates provided by the sub-block-based system using sub-block of 6×6 pixels applied to images of set A.

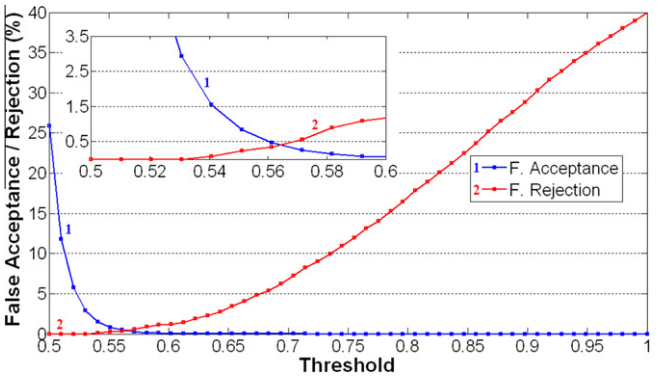

Fig. 19. False acceptance and false rejection rates provided by the sub-block-based system using sub-block of 4×4 pixels applied to images of set A.

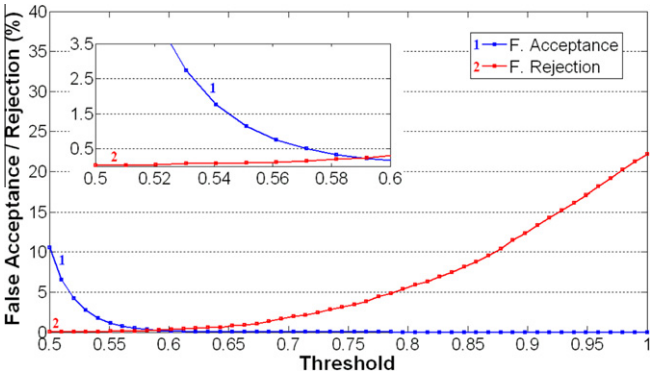

Fig. 20. False acceptance and false rejection rates provided by the sub-block system using the optimum sub-block applied to images of set A.

Table 3
Threshold values when the false acceptance and false rejection are equal, using sub-block-based eigenphases algorithm with different sub-block size together with conventional eigenphases method applied to images of set A.

Block size	F. acceptance/rejection (%)	Threshold
Complete image	2.12	0.516
12×12	1.02	0.537
6×6	0.45	0.561
4×4	0.41	0.564
2×2 (optimum)	0.23	0.591

rates decrease when a larger threshold is used, however in this situation the false rejection rates increase. However there is a point where the false acceptance and false rejection rates are equal, as shown in the amplified section of each figure. From this point, a larger threshold provides a larger false rejection rates while a smaller threshold value provides a larger false acceptation rates. Thus, by knowing the information provided by these figures an appropriate threshold for a specific application can be chosen, considering that when trying to get a lower false acceptance rate will result in the increase of false rejection rate.

From these figures we can point out that when the sub-block-based system with sub-block size of 2×2 pixels is used it is possible to achieve, simultaneously, a false acceptance and false rejection rate lower than 0.5%. This performance is not possible to obtain using the conventional eigenphases method because if we require a false acceptance rates lower than 0.5% the false rejection rate becomes higher than 2.5% and if a false rejection rate lower than 0.5% is desired, the false acceptance rate becomes higher than 5%. Then we can conclude that, in verification task, the sub-block-based system outperforms the conventional eigenphases method.

Table 3 shows the value of the threshold in which the false acceptance and false rejection rates are equal for the conventional eigenphases method, as well as the sub-block-based system using sub-block sizes of 12×12, 6×6, 4×4 as well as the optimum block size, 2×2 pixels. Here, it can be observed that the lowest false acceptance and rejection rates are obtained, with the sub-band-based system using the optimum sub-block size, which is approximately 2% lower than the conventional eigenphases method. We can conclude that when the optimum sub-block size is used the verification performance improves with respect to the conventional and other previously proposed sub-block-based eigenphases methods.

5. Conclusions

This paper presented a theoretical analysis of the effect of using sub-block processing in the eigenphases algorithm to obtain that the optimum sub-block size of a sub-block-based eigenphases algorithm, which achieves a significant improvement in both person classification and identity verification tasks. In the sub-block-based eigenphases algorithm the face image under analysis, firstly, is divided into sub-blocks of $N \times N$ pixels. Next the phase spectrum of each sub-block is independently calculated before applying the PCA to estimate the features vector; which is then applied to the SVM to perform, either, the identification or verification task. Theoretical and computer evaluation results show that the optimal sub-block size providing the better performance is equal to 2×2 pixels since, doing it, the performance of the sub-block-based method becomes almost independent of the illumination and facial expression conditions as well as partial occlusion.

To compare the performance of the conventional and sub-block-based eigenphases methods, under controlled conditions, the AR Face Database was used. The evaluation results show that the highest identification rate and lowest standard deviation is obtained when the optimum sub-block size, i.e. 2×2 pixels, is used. These results also show that the sub-block-based approach, considerably overcome the performance of conventional eigenphases method. It is important to mention again that the sub-block-based system performs better than the conventional eigenphases method, in particular using the optimum sub-block size, when both are required to identify faces with partial occlusion; since the sub-block-based algorithm provides a recognition rate of 97.2% while the recognition rate of the conventional one is about 85.4%. It is worth noting that even with significant partial occlusion in the testing images the performance of sub-block-based method, with optimum sub-block size, degrades only approximately 2% compared with 11% of the conventional one.

The sub-block-based and conventional approaches were also evaluated when they are required to perform verification tasks. In this situation using the sub-block-based approach, with optimum sub-block size, it is possible to achieve, simultaneously, a false acceptance and false rejection rates lower than 0.5%; performance that it is not possible to obtain using the conventional eigenphases method because to achieve a false acceptance rate lower than 0.5% the false rejection rate must be increased to about 2.5%; while if a false rejection rate lower than 0.5% is desired, the false acceptance rate becomes higher than 5%. Then we can conclude that the sub-block-based system outperforms the conventional eigenphases method when it is required to carry out either, identification or verification task, specially using a block size of 2×2 pixels that, according to theoretical and computer evaluation results can be considered as the optimum block size.

Acknowledgment

We thank the National Science and Technology Council of Mexico (CONACyT) and the National Polytechnic Institute of Mexico for the financial support during the realization of this research.

References

[1] S.Y. Kung, M.W. Mak, S.H. Lin, in: J. Peters (Ed.), Biometric Authentication: A Machine Learning Approach, second ed., vol. 3., Prentice Hall, New York, 2005, pp. 1–8. 85–131.
[2] H.M. El-Bakry, N. Mastorakis, Personal identification through biometric technology, in: 9th WSEAS International Conference on Applied Informatics and Communications (AIC '09), Moscow, Russia, 2009, pp. 325–340.
[3] Stan Z. Li, Anil K. Jain, Handbook of Face Recognition, Springer, 2005. pp. 1–13.
[4] R. Chellapa, P. Sinha, P.J. Phillips, Face recognition by computers and humans, Computer Magazine 43 (February) (2010) 46–55.
[5] Y. Gao, K.H. Maylor, Face recognition using line edge map, IEEE Transactions on Pattern Analysis and Machine Intelligence 24 (2002) 764–769.
[6] R. Gottumukkal, V.K. Asari, An improved face recognition technique based on modular PCA approach, Pattern Recognition Letters 25 (2004) 429–436.
[7] Haifeng Hu, Variable lighting face recognition using discrete wavelet transform, Pattern Recognition Letters 32 (13) (2011) 1526–1534. ISSN: 0167-8655.
[8] Hamidreza Rashidy Kanan, Karim Faez, GA-based optimal selection of PZMI features for face recognition, Applied Mathematics and Computation 205 (2008) 706–715.
[9] Ognjen Arandjelovic, Roberto Cipolla, A methodology for rapid illumination-invariant face recognition using image processing filters, Computer Vision and Image Understanding 113 (2009) 159–171.
[10] K. Hotta, Robust face recognition under partial occlusion based on support vector machine with local Gaussian summation kernel, Image and Vision Computing 26 (2008) 1490–1498.
[11] M. Sharkas, Application of DCT blocks with principal component analysis for face recognition, in: 5th WSEAS International Conference on Signal, Speech and Image Processing, 2005, pp. 107–111.
[12] Saeed Dabbagh chian, Masoumeh P. Ghaemmaghami, Ali Aghagolzadeh, Feature extraction using discrete cosine transform and discrimination power analysis with a face recognition technology, Pattern Recognition 43 (4) (2010) 1431–1440. ISSN: 0031-3203.
[13] Pei Zong Lee, Gau-Shin Liu, An efficient algorithm for the 2-D discrete cosine transform, Signal Processing 55 (2) (1996) 221–239. ISSN: 0165-1684.
[14] J. Olivares-Mercado, G. Sanchez-Perez, M. Nakano-Miyatake, H. Perez-Meana, Feature extraction and face verification using Gabor and Gaussian mixture models, Advances on Artificial Intelligence 4827 (2007) 769–778.

[15] G. Aguilar-Torres, K. Toscano-Medina, G. Sanchez-Perez, M. Nakano-Miyatake, H. Perez-Meana, Eigenface–Gabor algorithm for feature extraction in face recognition, International Journal of Computers 3 (2009) 20–30.
[16] Lin-Lin Huang, Akinobu Shimizu, Hidefumi Kobatake, Robust face detection using Gabor filter features, Pattern Recognition Letters 26 (11) (2005) 1641–1649. ISSN: 0167-8655.
[17] R. Thiyagarajan, S. Arulselvi, G. Sainarayanan, Gabor feature based classification using statistical models for face recognition, Procedia Computer Science 2 (2010) 83–93. ISSN: 1877-0509.
[18] D. Dao-Qing, Y. Hong, Wavelets and face recognition, in: Face Recognition, I-Tech, Vienna, 2007, pp. 59–74.
[19] A. Eleyan, H. Ozkaramanli, H. Demirel, Complex wavelet transform based face recognition, EURASIP Journal on Advances in Signal Processing 2008 (2008).
[20] Kresimir Delac, Mislav Grgic, Sonja Grgic, Face recognition in JPEG and JPEG2000 compressed domain, Image and Vision Computing 27 (2009) 1108–1120.
[21] P.C. Mali, B.B. Chaudhuri, D. Dutta Majumder, Properties and some fast algorithms of the Haar transform in image processing and pattern recognition, Pattern Recognition Letters 2 (5) (1984) 319–327. ISSN: 0167-8655.
[22] Xiao-ning Song, Yu-jie Zheng, Xiao-jun Wud, Xi-bei Yang, Jing-yu Yang, A complete fuzzy discriminant analysis approach for face recognition, Applied Soft Computing 10 (2010) 208–214.
[23] Mehmet Koc, Atalay Barkana, A new solution to one sample problem in face recognition using FLDA, Applied Mathematics and Computation 217 (2011) 10368–10376.
[24] L. Sirovich, M. Kirby, Low-dimensional procedure for the characterization of human faces, Journal of the Optical Society of America A 4 (3) (1987) 519–524.
[25] M. Turky, A. Pentland, Eigenphaces for recognition, Journal of Cognitive Neuroscience 3 (1) (1991) 71–86.
[26] M. Savvides, B.V.K. Vijaya Kumar, P.K. Khosla, Eigenphases vs. eigenphaces, in: Proceedings of the 17th International Conference on Pattern Recognition, ICPR, vol. 3, August 2004, pp. 810–813.
[27] Jesus Olivares-Mercado, Gualberto Aguilar, Karina Toscano-Medina, Mariko Nakano, Hector Perez Meana, in: Peter M. Corcoran (Ed.), GMM vs. SVM for Face Recognition and Face Verification, Reviews, Refinements and New Ideas in Face Recognition, 2011, ISBN: 978-953-307-368-2, InTech, <http://www.intechopen.com/articles/show/title/gmm-vs-svm-for-face- recognition-and-face-verification>.
[28] Slobodan Ribaric, Marijo Maracic. Eigenphase-based face recognition: a comparison of phase information extraction methods, in: Proceedings of the Nineteenth International Electrotechnical and Computing Science Conference ERK 2010, Slovenian Section IEEE 2010, 2010, pp. 233–236.
[29] J. Olivares-Mercado, K. Hotta, H. Takahashi, H. Perez-Meana, G. Sanchez-Perez, Face recognition based on the phase spectrum of local normalized image, in: MICAI Proceedings of MICAI, 2008, pp. 123–127.
[30] J. Olivares-Mercado, K. Hotta, H. Takahashi, M. Nakano-Miyatake, K. Toscano-Medina, H. Perez-Meana, Improving the eigenphase method for face recognition, IEICE Electronic Express 6 (2009) 1112–1117.
[31] K. Ramirez-Gutierrez, D. Cruz-Perez, J. Olivares-Mercado, M. Nakano-Miyatake, H. Perez-Meana, A face recognition algorithm using eigenphases and histogram equalization, International Journal of Computers 5 (1) (2011) 34–41.
[32] Gibran Benitez-Garcia, Jesus Olivares-Mercado, Gualberto Aguilar-Torres, Gabriel Sanchez-Perez, Hector Perez-Meana, Face identification based on contrast limited adaptive histogram equalization (CLAHE), in: Proceedings of the International Conference on Image Processing, Computer Vision, and Pattern Recognition (IPCV'11), WORLDCOMP'11, Nevada, USA, July 2011, ISBN: 1-60132-191-0.
[33] Rafael C. Gonzalez, Richard E. Woods, Digital Image Processing, third ed., Pearson Prentice Hall, 2008. pp. 120–128.
[34] S.M. Pizer, E.P. Amburn, J.D. Austin, R. Cromartie, A. Geselowitz, T. Greer, B.M. terHaarRomeny, J.B. Zimmerman, K. Zuiderveld, Adaptive histogram equalization and its variations, Computer Vision, Graphics and Image Processing 39 (1987) 355–368.
[35] K. Zuiderveld, Contrast limited adaptive histogram equalization, in: P.S. Heckbert (Ed.), Graphics Gems IV, Academic Press, Cambridge, MA, 1994, pp. 474–485 (Chapter VIII.5).
[36] Ali M. Reza, Realization of the contrast limited adaptive histogram equalization (CLAHE) for real-time image enhancement, Journal of VLSI Signal Processing 38 (2004) 35–44.
[37] Zhiyuan Xu, Xiaoming Liu, Na Ji, Fog removal from color images using contrast limited adaptive histogram equalization, in: 2nd International Congress on Image and Signal Processing 2009, October 2009, pp 1–5.
[38] M.H. Hayes, J.S. Lim, A.V. Oppenheim, Signal reconstruction from phase or magnitude, IEEE Transactions 28 (1980) 672–680.
[39] A.V. Oppenheim, J.S. Lim, The importance of phase in signals, in: Proc. IEEE, vol. 69, May 1981, pp. 529–541.
[40] J. Shlens, A Tutorial on Principal Component Analysis, Center of Neural Science, New York University and Systems Neurobiology Laboratory, Salk Institute for Biological Studies, April 2009.
[41] Ya Xiong Zhang, Artificial neural networks based on principal component analysis input selection for clinical pattern recognition analysis, Talanta, 0039-9140 73 (1) (2007) 68–75.
[42] Tom Howley, Michael G. Madden, Marie-Louise O'Connell, Alan G. Ryder, The effect of principal component analysis on machine learning accuracy with high-dimensional spectral data, Knowledge-Based Systems 19 (5) (2006) 363–370. ISSN: 0950-7051.
[43] Harun Uğuz, A two-stage feature selection method for text categorization by using information gain, principal component analysis and genetic algorithm, Knowledge-Based Systems 24 (7) (2011) 1024–1032. ISSN: 0950-7051.
[44] Guan-Chun Luh, Chun-Yi Lin, PCA based immune networks for human face recognition, Applied Soft Computing 11 (2011) 1743–1752.
[45] G. Costantini, D. Casali, T. Massimiliano, An SVM based classification method for EEG signals, in: Proceedings of the 14th WSEAS International Conference on Circuits, 2010, pp. 107–109.
[46] Juan José Rodríguez, Carlos J. Alonso, José A. Maestro, Support vector machines of interval-based features for time series classification, Knowledge-Based Systems 18 (4–5) (2005) 171–178. ISSN: 0950-7051.
[47] Chih-Chung Chang, Chih-Jen Lin, LIBSVM: a library for support vector machines, ACM Transactions on Intelligent Systems and Technology 2 (2011) 27:1–27:27.
[48] Jin Chang Ren, ANN vs. SVM: which one performs better in classification of MCCs in mammograming, Knowledge-Based Systems 26 (2012) 144–153. ISSN: 0950-7051.
[49] W.M. Campbell, J.P. Campbell, D.A. Reynolds, E. Singer, P.A. Torres-Carrasquillo, Support vector machines for speaker and language recognition, Computer Speech and Language 20 (2–3) (2006) 210–229.
[50] Weihong Li, Lijuan Liu, Weiguo Gong, Multi-objective uniform design as a SVM model selection tool for face recognition, Expert Systems with Applications 38 (2011) 6689–6695.
[51] The AR face database. <http://www.ece.osu.edu/aleix/ARdatabase.html>.